Universidade Federal Rural do Semi-Árido
Pró-Reitoria de Pesquisa e Pós-Graduação
https://periodicos.ufersa.edu.br/index.php/caatinga

ISSN 0100-316X (impresso)
ISSN 1983-2125 (online)
http://dx.doi.org/10.1590/1983-21252021v34n119rc

MULTIFRACTAL ANALYSIS OF SOIL RESISTANCE TO PENETRATION IN DIFFERENT PEDOFORMS[1]

JAIRO OSVALDO RODRIGUEZ LEIVA[2], RAIMUNDA ALVES SILVA[2], ÊNIO FARIAS DE FRANÇA E SILVA[3], GLÉCIO MACHADO SIQUEIRA[4]*

ABSTRACT - Soils are highly variable across landscapes, which can be assessed and characterized according to scale, as well as fractal and multifractal concepts of scale. Thus, the objective of this study was to analyze the multifractality of the penetration resistance (PR) of vertical profiles from different slope forms (concave and convex). The experimental plot incorporated 44.75 ha, and the PR was measured at 70 sampling points in the 0-0.6 m layer, distributed in concave (Type A: 38 sampling points) and convex pedoforms (Type B: 32 sampling points). Data analysis was performed using the PR value (every 0.01 m depth) for each of the sampling points (PR_{mean}), and their respective maximum ($PR_{maximun}$) and minimum ($PR_{minimum}$) values. Multifractal analysis was performed to assess the changes in the structure, heterogeneity, and uniformity of the vertical profiles according to the scale, characterizing the partition function, generalized dimension, and singularity spectrum. The multifractal parameters of the generalized dimension and singularity spectrum demonstrated greater homogeneity and uniformity in the vertical PR profiles of pedoform B (convex) compared to those of pedoform A (concave). The minimum PR values in pedoform A ($PR_{minimum}$) showed the greatest scale heterogeneity, indicating that in terms of soil management, it is more relevant to monitor the minimum values than the maximum values. The fractal analysis allowed us to describe the heterogeneity of the data on scales not evaluated by conventional analysis methods, with high potential for use in precision agriculture and the delimitation of specific management zones.

Keywords: Scale heterogeneity. Precision agriculture. Soil compaction. Soil management. Spatial variability.

ANÁLISE MULTIFRACTAL DA RESISTÊNCIA DO SOLO À PENETRAÇÃO EM DIFERENTES PEDOFORMAS

RESUMO – Os solos possuem elevada variabilidade ao longo da paisagem, que pode ser avaliada e caracterizada por meio de conceitos de invariância de escala, fractais e multifractais. Assim, o objetivo deste trabalho foi analisar a multifractalidade da RP de perfis verticais em diferentes formas do relevo (côncavo e convexo). A parcela experimental possui 44,75 ha, e a resistência à penetração (RP) foi medida em 70 pontos de amostragem na camada de 0-0,6 m, distribuídos nas pedoformas côncava (Tipo A: 38 pontos de amostragem) e convexa (Tipo B: 32 pontos de amostragem). A análise dos dados foi realizada utilizando o valor de RP a cada 0,01 m para os pontos de amostragem (RP_{media}), e seus respectivos valores máximos (RP_{maxima}) e mínimos (RP_{minimo}). A análise multifractal foi realizada para se avaliar as mudanças na estrutura, heterogeneidade e uniformidade dos perfis verticais por meio da propriedade de escala, caracterizando a função de partição, a dimensão generalizada e o espectro de singularidade. Os parâmetros multifractais da dimensão generalizada e do espectro de singularidade demonstraram maior homogeneidade e uniformidade dos perfis verticais de RP na pedoforma Tipo B (convexa), quando comparado a pedoforma A (côncava). Os valores de $RP_{mínimo}$ na pedoforma A apresentaram a maior heterogeneidade de escala, indicando que em termos de manejo do solo, o monitoramento dos valores mínimos é mais relevante que os valores máximos. A análise fractal permitiu descrever a heterogeneidade dos dados em escalas não avaliadas pelos métodos análise convencionais, com elevado potencial para a prática da agricultura de precisão e delimitação de zonas de manejo específico.

Palavras-chave: Heterogeneidade de escala. Agricultura de precisão. Compactação do solo. Manejo do solo. Variabilidade espacial.

*Corresponding author
[1]Received for publication in 11/25/2019; accepted in 10/26/2020.
Paper extracted from the doctoral thesis of the first author.
[2]Postgraduate Program in Biodiversity and Biotechnology-BIONORTE, Universidade Federal do Maranhão, São Luís, MA, Brazil; leivaagro@gmail.com – ORCID: 0000-0002-1803-2241, ray-234@hotmail.com – ORCID: 0000-0002-0380-8190.
[3]Postgraduate Program in Agricultural Engineering, Universidade Federal Rural de Pernambuco, Recife, PE, Brazil; effsilva@uol.com.br - ORCID: 0000-0002-8652-503X.
[4]Postgraduate Program in Geography, Universidade Federal do Maranhão, São Luís, MA, Brazil; gleciosiqueira@hotmail.com – ORCID: 0000-0002-3513-2658.

INTRODUCTION

Knowledge of soil resistance to penetration (PR, MPa) allows inferences concerning the state of soil compaction throughout the landscape and the determination of management alternatives with the least possible impact on soil attributes, especially with regard to increasing density and decreasing soil porosity (SOUZA et al., 2015; BURR-HERSEY et al., 2017; SEIDEL et al., 2018). Thus, the understanding of PR along the landscape is a key factor for the development of management alternatives with less impact on natural soil characteristics (SIQUEIRA et al., 2013), in addition to favoring the development of crops (SEIDEL et al., 2018).

According to Goovaerts (1998), variability is composed of defined or intrinsic variations and random fluctuations or noise, which need to be understood individually to facilitate a better understanding of the processes and dynamics of soil properties throughout the landscape. In this way, knowledge of landscape forms allows us to describe the variability of soil attributes and their relationships with crops at different scales. Logsdon, Perfect and Tarquis (2008) highlighted that the distinction between intrinsic variability and noise depends upon the measurement scale, and that an increase in the observation scale almost always has a noise structure. Therefore, it is necessary to understand the scales of variation across landscapes. In this sense, Leão et al. (2011) studied the spatial variability of soil attributes, including the PR of different slope forms, and found the greatest differences for the concave slope compared to the convex slope. In addition, Siqueira et al. (2018) indicated that relief forms can be used to predict and improve the estimation of soil attributes. When studying vertical PR profiles using multifractal analysis, Leiva et al. (2019) found that the heterogeneity and variability of this attribute is influenced by its position in the landscape. Therefore, it is necessary to understand how PR varies across the landscape in the context of the occurrence of different patterns on the horizontal and vertical scales, especially over small distances (KRAVCHENKO; PACHEPSKY, 2004).

In this sense, multifractal analysis aims to determine variations in different compartments according to the scale (VIDAL-VÁZQUEZ et al., 2013; LEIVA et al., 2019). In this way, it is possible to conduct an in-depth study of PR profiles with high variability through the study of different compartments, which differ and present scale heterogeneity (SIQUEIRA et al., 2013). Roisin (2007) evaluated PR using multifractal analysis to understand the state of soil structure. Siqueira et al. (2013) studied the multifractality and intrinsic variability of vertical PR profiles in soils with a high water content. Wilson et al. (2016) studied the influence of water deficit on the multifractal structure of vertical PR profiles. Overall, it is apparent that few studies have been dedicated to the study of the fractal and multifractal geometry of the PR data of different slope forms.

Thus, the hypothesis of this study was that PR measurements along the landscape vary according to the shape of the slope. The objective of this study was to analyze the multifractality of PR in the vertical profiles of different slope forms (concave and convex) in an area cultivated with soybean under no-tillage conditions.

MATERIALS AND METHODS

The study area incorporates approximately 44.75 ha and is located in the municipality of Mata Roma (Maranhão, Brazil; 3º 70'80.88” S and 43º 18'71.27” W). The climate is Aw (hot and humid tropical), with an average annual temperature above 27 °C and average annual rainfall of 1,835 mm, with concentrated rains from January to June. The soil in the study area is anoxisol (SANTOS et al., 2018), and its main physical and chemical characteristics are shown in Table 1.

In the study area, soybean (*Glicine max* L.) and corn (*Zea mays* L.) have been cultivated in rotation since 2007, under a no-tillage system. Subsoiling, up to a depth of 0.32 m, is completed every five years. In the 2015/16 agricultural year, 70 sampling points were marked in the study area following the planting lines, with a regular spacing of 100 × 35 m (Figure 1). The points were georeferenced using GPS with post-processed differential correction (DGPS). The area has a smooth wavy slope with two slope units: concave (Type A: slope between 101.8-103.8 m; 38 sampling points) and convex (Type B: slope between 103.8-105.8 m; 32 sampling points) (Figure 1).

The resistance of the soil to penetration (PR, MPa) was determined on 04/22/2016 using an impact penetrometer, with a cone angle of 30°. The PR was evaluated in the 0-0.6 m depth layer. Values were calculated for each 0.01 m.

For the purpose of verifying the greatest differences in the PR readings across the 70 sampling points and pedoforms (A and B), we used the average (PR_{mean}), maximum ($PR_{maximum}$), and minimum ($PR_{minimum}$) PR values of the vertical profiles at 0.01 m intervals, which were submitted to multifractal analysis. The PR readings were recorded when the soil was at field capacity (0.171 m^3 m^{-3} for the 70 sampling points, 0.172 m^3 m^{-3} for the Type A pedoform, and 0.172 m^3 m^{-3} for the Type B pedoform), which was determined using a Richards chamber.

Table 1. Physical and chemical characterization of the soil cultivated with soybean under no-tillage conditions.

0-0.2 m													
Sand	Silt	Clay	SD	Macro	Micro	TP	OM	pH	P	K	Ca	Mg	CEC
-------- g kg^{-1} -----------			mg m^{-3}	--------- m^3 m^{-3} ---------			g dm^{-3}		mg dm^{-3}	---------- $mmol_c$ dm^{-3} ----------			
745.58	138.214	117.143	1.268	0.169	0.378	0.547	22	5	49	0.7	18	3	46.7
0.2-0.4 m													
Sand	Silt	Clay	SD	Macro	Micro	TP	OM	pH	P	K	Ca	Mg	CEC
-------- g kg^{-1} ---------			mg m^{-3}	--------- m^3 m^{-3} ----------			g dm^{-3}		mg dm^{-3}	---------- $mmol_c$ dm^{-3} ----------			
737.772	141.7	120.629	1.291	0.16	0.372	0.532	19	4.7	47	0.5	17	3	45.6

SD: soil density; Macro: macroporosity; Micro: microporosity; TP: total porosity; OM: organic matter; CEC: cation exchange capacity.

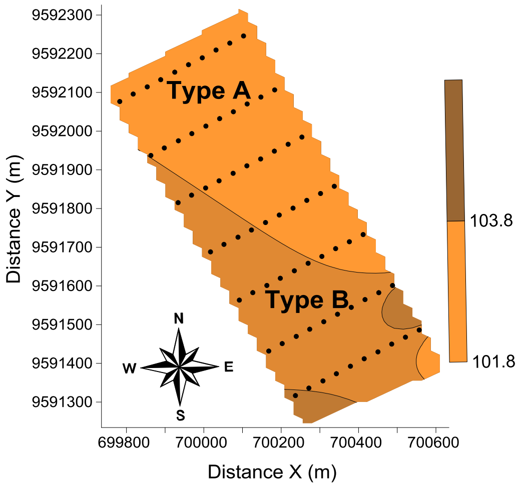

Figure 1. Slope map of the study area showing the concave (Type A) and convex (Type B) pedoforms and the geographical location of the 70 sampling points (100 × 35 m spacing).

Data were analyzed using descriptive statistics in the R 3.3.1 software (R CORE TEAM, 2018). The following measurements were determined: mean, variance, standard deviation, coefficient of variation, asymmetry, kurtosis, and D (maximum deviation in relation to normal distribution, using the Kolmogorov-Smirnov test with an error probability of 0.01).

The multifractal analysis was performed for each vertical PR profile using the moment method with consideration for the scale, allowing for the determination of the partition function, generalized dimension, and singularity spectrum, according to the procedures described by Evertsz and Mandelbrot (1992). The algorithms used in this study are shown in Table 2.

The partition function was built for successive segments in 2^k, k = 0 to k = 6, and moments in the range of q = +5 to q = -5 (EVERTSZ; MANDELBROT, 1992), generalizing on a δ scale to a number of segments $N(\delta) = 2^k$ of characteristic size, $\delta = L \times 2^{-k}$, which corresponded to the length of the vertical PR profiles (0.6 m). The probability of the mass function, Pi (δ) (Equation 1a), describes the value of the segment [Ni (δ)] and the sum of the measure across the transept [N_t], with q defined as $-\infty < q < \infty$. This enabled the evaluation of the segment sizes, n (δ) in normalized scale μi (δ), according to Equation 1b, which allowed the plotting of χ (q, δ) versus δ. Then, the exponent of the mass function [τ (q) - Equation 1c] was determined.

The scale function (τ_q) is related to the generalized fractal dimension (HENTSCHEL; PROCACCIA, 1983), and was defined in Equation 2a. The generalized dimension (Dq) or Rényi dimension of order q was also determined using Equation 2b. In this case, D1 was undetermined because the denominator value was equal to zero. However, Equation 2c was used for q = 1, which enabled the determination of the moment dimensions q = 0, q = 1, and q = 2 (called the capacity dimension (D_0), entropy dimension or Shannon's entropy (D_1), and correlation dimension (D_2), respectively) (HENTSCHEL; PROCACCIA, 1983).

The singularity spectrum was determined using Equations 3a and 3b. Here, it is necessary to consider that in multifractal measures, the number [N_δ (α)] of cells of size δ with a singularity or Hölder exponent equal to α increase or decrease with δ. In this case, it obeys a power law: $N(\alpha)$ $\alpha\delta^{-f(\alpha)}$, which describes exponent $f(\alpha)$ as a continuous function of α. The graph depicting the typical singularity spectrum has a descending concave parabola shape, where the α values increase as a function of the heterogeneity of the measurements. The scaling of the exponents τ_q and $f(\alpha)$ can be obtained through the transformation of Legendre; however, the present study uses Chhabra and Jensen (1989) (Equations 3a and 3b).

Table 2. Equations used for the multifractal analysis.

	Equations	
Partition function	$p_i(\delta) = \frac{N_i(\delta)}{N_t}$	(1a)
	$\chi(q,\delta) = \sum_{i=1}^{n(\delta)} p_i^q(\delta)$	(1b)
	$\tau(q) = \lim_{\delta\to 0} \frac{\log\chi(q,\delta)}{\log(1/\delta)}$	(1c)
Generalized dimension (Dq)	$D_q = \tau(q)/(q-1)$	(2a)
	$D_q = \frac{1}{q-1}\lim_{\delta\to 0}\frac{\log[\chi(q,\delta)]}{\log\delta} = \frac{\tau(q)}{q-1}$ para $q \neq 1$	(2b)
	$D_1 = \lim_{\delta\to 0}\frac{\sum_{i=1}^{n(\delta)} p_i(\delta)\log[p_i(\delta)]}{\log\delta}$ para $q = 1$	(2c)
Singularity spectrum	$\alpha(q) \propto \frac{\sum_{i=1}^{N(\delta)} \mu_i(q,\delta)\log[p_i(\delta)]}{\log(\delta)}$	(3a)
	$f(\alpha(q)) \propto \frac{\sum_{i=1}^{N(\delta)} \mu_i(q,\delta)\log[\mu_i(q,\delta)]}{\log(\delta)}$	(3b)

RESULTS AND DISCUSSION

There was an increase in the PR close to the 0.3 m soil depth, with the highest average PR value of the Type B pedoform being 3.052 MPa, while that of the Type A pedoform was 3.718 MPa. The highest average PR value for the 70 sampling points (pedoform A and B) was 3.345 MPa. According to Cortez et al. (2018), Seidel et al. (2018), and Leiva et al. (2019), high PR values are related to soil management, and crops in no-tillage systems need management strategies that consider the state of soil compaction (BURR-HERSEY et al., 2017). The Type A slope unit (concave; Figures 1 and 2b) showed the highest average PR value (3.718 MPa) and highest variation of the standard deviation along the profile, indicating the high vertical variability of the data. Leão et al. (2011) highlighted that soil attributes have greater variability in concave slope units.

The statistical analysis of the PR_{mean}, $PR_{maximum}$, and $PR_{minimum}$ for the vertical PR profiles (Table 3) demonstrated that the lowest PR_{mean} value occurred in the Type B slope (PR_{mean} = 2.277 MPa), followed by the 70 sampling points (PR_{mean} = 2.333 MPa) and the Type A slope (PR_{mean} = 2.374 MPa). Similarly, this pattern was repeated for the $PR_{maximum}$ values. For the $PR_{minimum}$ values, the lowest mean value occurred in the 70 sampling points (PR = 0.852 MPa), followed by the Type A (PR = 0.914 MPa) and Type B (PR = 0.935 MPa) pedoforms. Thus, we found that the analysis of the PR for the 70 sampling points underestimates the average PR values (Table 3).

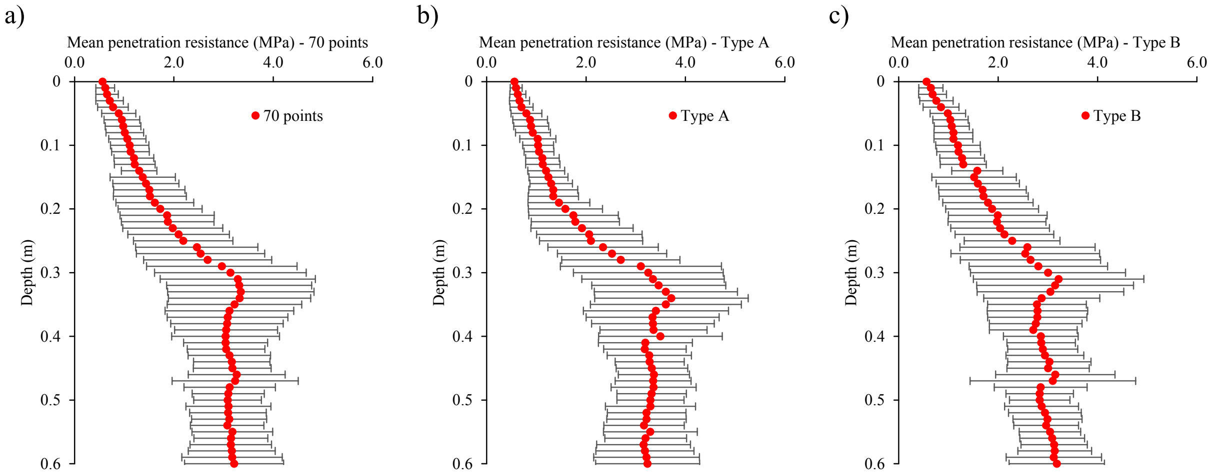

Figure 2. Average PR value and standard deviation for the 70 sampling points (a), Type A pedoform (b), and Type B pedoform (c) in the study area cultivated with soybean under no-tillage conditions.

Table 3. Descriptive statistics for the soil resistance to penetration of the three units

	------------- 70 points ------------			------------- Type A -----------			------------- Type B ------------		
	Mean	Maximum	Minimum	Mean	Maximum	Minimum	Mean	Maximum	Minimum
Mean	2.333	4.801	0.852	2.374	4.533	0.914	2.277	4.355	0.935
Variance	0.922	4.855	0.153	1.175	4.597	0.239	0.710	3.652	0.186
Standard deviation	0.960	2.203	0.391	1.084	2.144	0.489	0.843	1.911	0.431
CV %	41.168	45.890	45.864	45.648	47.303	53.518	37.021	43.886	46.104
Asymmetry	-0.545	-0.078	1.715	-0.418	-0.041	1.881	-0.665	-0.051	1.022
Kurtosis	-1.373	-0.917	1.819	-1.568	-0.896	2.204	-1.068	-0.537	-0.454
D	0.278Ln	0.136n	0.396Ln	0.274Ln	0.161n	0.438Ln	0.224Ln	0.132n	0.36Ln

D: Maximum deviation from the normal distribution using the Kolmogorov–Smirnov test with an error probability of 0.01.

The lowest value for the coefficient of variation (CV) was described for the Type B pedoform (CV = 37.021%), followed by the 70 sampling points (CV = 41.168%) and Type A pedoform (CV = 45.648%). The differences in the CV values demonstrate the need for a separate study of PR measurements, since the difference between the lowest and highest mean CV values is approximately 8%, which corroborates the results of Roisin (2007) and Leiva et al. (2019). It is important to highlight that PR measurements have a high intrinsic variability, as PR is influenced by changes along the soil profile, particularly those related to clay content, moisture, density, and porosity (SIQUEIRA ET AL., 2013; BURR-HERSEY et al., 2017; SEIDEL et al., 2018), thus being a variable with high variability, resulting in high CV values.

According to the Kolmogorov-Smirnov data normality test ($p < 0.01$), the $PR_{maximum}$ for the 70 sampling points and Type B pedoform showed a normal frequency distribution, while the other data showed a lognormal frequency distribution.

The graph was constructed considering segments 2^k, k = 0 to k = 6, with determination coefficients (R^2) greater than 0.9. The $PR_{maximum}$ presented different adjustment values for the partition function graphs of pedoforms A (R^2 = 0.999; Figure 3e) and B (R^2 = 0.996; Figure 3h). The partition function graphs of PR_{mean} were adjusted with R^2 = 0.999 (Figures 3a, d, and g), while those of $PR_{minimum}$ were adjusted with R^2 = 0.998 (Figures 3c, f, and i). Visually, the $PR_{minimum}$ graphs for the 70 sampling points (Figure 3c) and pedoform A (Figure 3f) show greater data variability in the range of q = 5 to q = -5. Morató et al. (2017), studying the multifractality of physical soil variables, presented a graph of the partition function with behavior similar to that found in this study for the $PR_{minimum}$. The variations in the moments reflected the data variability, since $PR_{minimum}$ had the highest CV values (%; Table 3). In this way, the partition functions for the PR (Figure 3) under soybean cultivation in a no-tillage system were characterized on multiple scales, that is, multifractal scales obeying a power law, as described by Banerjee et al. (2011), Siqueira et al. (2018), and Wilson et al. (2016).

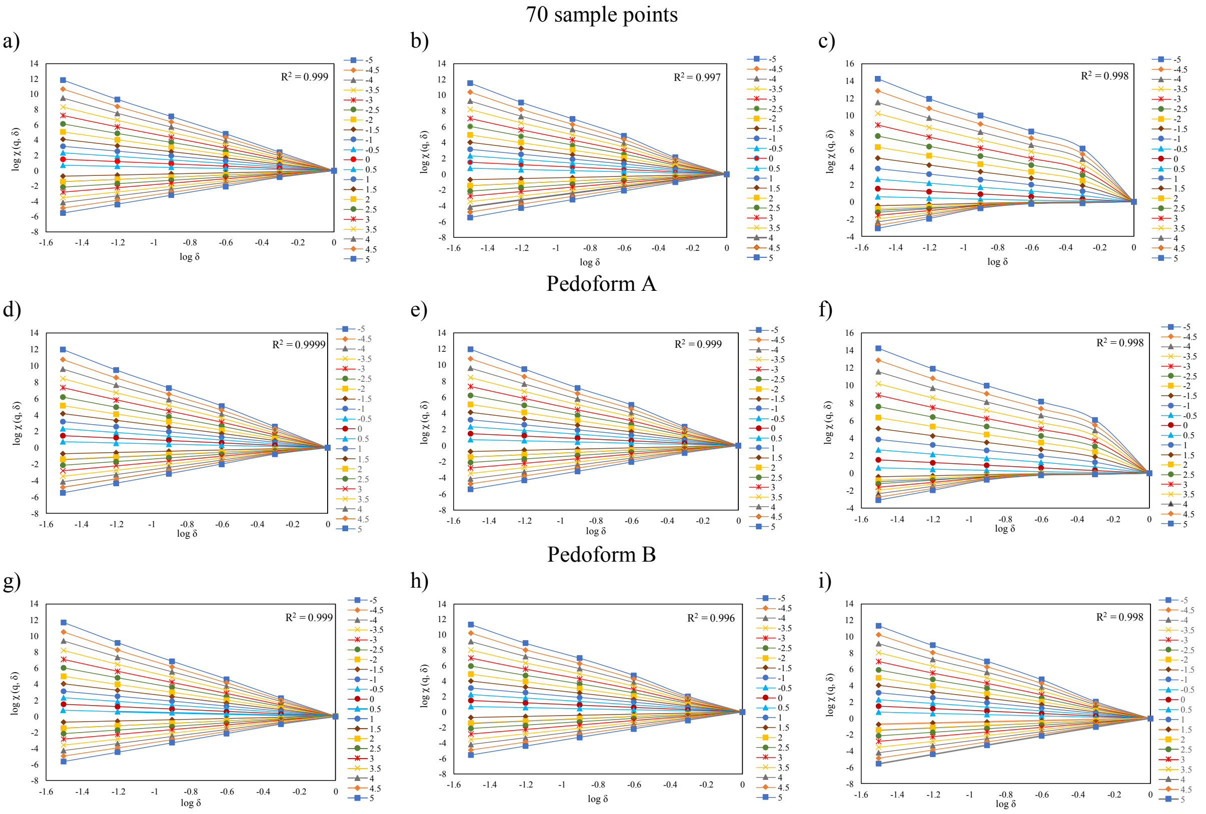

Figure 3. Partition function χ (q, δ) for the resistance of soil to penetration in the 70 sample points [PR_{mean} (a), $PR_{maximum}$ (b), and $PR_{minimum}$ (c)], Pedoform A [PR_{mean} (d), $PR_{maximum}$ (e), and $PR_{minimum}$ (f)], and Pedoform B [PR_{mean} (g), $PR_{maximum}$ (h), and $PR_{minimum}$ (i)] under soybean cultivation.

The smallest difference values between D_{-5}-D_5 are 0.340 (PR_{mean}) and 0.333 ($PR_{maximum}$ and $PR_{minimum}$) in pedoform B. According to Dafonte-Dafonte et al. (2015), the D_{-5}-D_5 difference is often used as an index of multifractality, meaning that pedoform B has different degrees of multifractality. The results indicate that the greater the adjustment of the partition function data, the greater the difference between D_{-5}-D_5 (Figure 3 and Table 4), indicating that the differences in the PR values at the different depths have variations that are explained and related to the soil management in the study area. Therefore, studies that facilitate the understanding of the multifractal dynamics of soil attributes are important, as they add new parameters to the decision-making process. However, it is necessary to consider that soils are not ideal fractals (KRAVCHENKO; PACHEPSKY, 2004), meaning that the decision-making process must consider the soil as a dynamic system and use different modeling tools.

The capacity dimension values (D_0; Table 4 and Figures 4a, b, and c) of the studied data are constant (D_0 = 1,000). D_0 provides global or average system information, and allows us to confirm the homogeneity of the data series being studied (PR_{mean}, $PR_{maximum}$, and $PR_{minimum}$). The information dimension or Shannon's entropy (D_1) quantifies the degree of distribution disorder, and must be in the range $0 < D_1 < 1$. Therefore, D_1 values close to 1 characterize a system uniformly distributed on all scales, while values close to 0 reflect a subset of scales in which irregularities are concentrated (VILLAS-BOAS; CRESTANA; POSADAS, 2014; Leiva et al., 2019). The PR data series describes uniformly distributed systems, with data ranging from 0.642 ($PR_{minimum}$ - 70 points) to 0.975 (PR_{mean} - pedoform B). It is worth mentioning that the PR in pedoform A presented the lowest D_1 values compared to those of the other data. The correlation dimension (D_2) computes the correlation of size intervals (L); that is, it is a geometric measure that describes the complexity of interval segments where the segments are correlated, so the larger the dimension, the larger the D_2 value. The highest D_2 values were described in pedoform B (PR_{mean} = 0.962; $PR_{maximum}$ = 0.955; and $PR_{minimum}$= 0.955), while pedoform A showed the lowest D_2 values (PR_{mean} = 0.948; $PR_{maximum}$ = 0.942; and $PR_{minimum}$ = 0.550).

The parameters of the singularity spectrum (q_-, q_+, α_0, α_5, and α_{-5}; Table 4) indicate that the data have variable amplitudes, according to the q_- and q_+

values (Table 4 and Figures 4d, e, and f). The Hölder exponent (α_0) quantifies the irregularity of the local density of a measurement (L) at any point in a multifractal system, and the smallest values (α_0) were associated with pedoform B (ranging from 1.032 ± 0.004 to 1.034 ± 0.006), followed by 70 sampling points (ranging from 1.038 ± 0.007 to 1.365 ± 0.124) and pedoform A (ranging from 1.044 ± 0.010 to 1.359 ± 0.123).

Table 4. Multifractal parameters obtained for the generalized dimension (D_{-10}-D_{10}, D_{-10}, D_{10}, D_0, D_1, and D_2) and singularity spectrum (q +, q-, α0, α_5, and α_{-5}).

Generalized dimension						
	D_{-5}-D_5	D_{-5}	D_5	D_0	D_1	D_2
70 points						
PR_{mean}	0.359	0.939 ± 0.020	1.297 ± 0.010	1.000 ± 0.000	0.971 ± 0.005	0.956 ± 0.011
$PR_{maximum}$	0.367	0.910 ± 0.008	1.278 ± 0.023	1.000 ± 0.000	0.968 ± 0.004	0.946 ± 0.006
$PR_{minimum}$	0.920	0.507 ± 0.104	1.427 ± 0.189	1.000 ± 0.000	0.642 ± 0.006	0.545 ± 0.090
Pedoform A						
PR_{mean}	0.377	0.930 ± 0.025	1.307 ± 0.019	1.000 ± 0.000	0.966 ± 0.008	0.948 ± 0.014
$PR_{maximum}$	0.410	0.910 ± 0.014	1.320 ± 0.019	1.000 ± 0.000	0.963 ± 0.004	0.942 ± 0.008
$PR_{minimum}$	0.921	0.511 ± 0.103	1.432 ± 0.186	1.000 ± 0.000	0.648 ± 0.068	0.550 ± 0.090
Pedoform B						
PR_{mean}	0.340	0.945 ± 0.016	1.285 ± 0.011	1.000 ± 0.000	0.975 ± 0.004	0.962 ± 0.008
$PR_{maximum}$	0.333	0.925 ± 0.006	1.258 ± 0.025	1.000 ± 0.000	0.972 ± 0.003	0.955 ± 0.005
$PR_{minimum}$	0.333	0.925 ± 0.006	1.258 ± 0.025	1.000 ± 0.000	0.972 ± 0.003	0.955 ± 0.005

Singularity spectrum					
	q_-	q_+	α_0	α_{-5}	α_5
70 points					
PR_{mean}	5.000	-4.000	1.038 ± 0.007	1.515 ± 0.022	0.927 ± 0.036
$PR_{maximum}$	5.000	-3.500	1.039 ± 0.007	1.461 ± 0.047	0.876 ± 0.014
$PR_{minimum}$	1.500	-5.000	1.365 ± 0.124	1.593 ± 0.297	0.532 ± 0.116
Pedoform A					
PR_{mean}	5.000	-4.000	1.044 ± 0.010	1.520 ± 0.036	0.917 ± 0.042
$PR_{maximum}$	5.000	-4.000	1.047 ± 0.007	1.539 ± 0.035	0.879 ± 0.025
$PR_{minimum}$	1.500	-5.000	1.359 ± 0.123	1.603 ± 0.292	0.536 ± 0.116
Pedoform B					
PR_{mean}	5.000	-3.500	1.032 ± 0.004	1.483 ± 0.030	0.933 ± 0.029
$PR_{maximum}$	5.000	-3.500	1.034 ± 0.006	1.432 ± 0.051	0.894 ± 0.009
$PR_{minimum}$	5.000	-3.500	1.034 ± 0.006	1.432 ± 0.051	0.894 ± 0.009

D_{-5}-D_5: difference between the maximum and minimum dimensions; D_5: maximum dimension; D_{-5}: minimum dimension; D_0: capacity dimension; D_1: entropy dimension; D_2: dimension of correlation.

The D_0, D_1, and D_2 values showed differences within the data series, which allowed us to characterize that the systems under study are multifractal. This was done in accordance with Banerjee et al. (2011), who stated that the dimensions must follow the trend of $D_0 > D_1 > D_2$ for an attribute to be multifractal. Therefore, the data series represents multifractal systems, and the data allowed us to describe changes in the dimension values of the different slope forms, showing that the PR samples are affected by the landscape changes.

Pedoform A showed the greatest amplitude (α_{-5}-α_5), with a PR_{mean} of 0.603, $PR_{maximum}$ of 0.66, and $PR_{minimum}$ of 1.067. The difference between α_{-5}-α_5 is an indicator of heterogeneity, with the greatest heterogeneity in this case associated with the $PR_{minimum}$ (Figure 4f). It is important to note that the $PR_{minimum}$ for 70 points and pedoform A describe greater heterogeneity/entropy, with α_{-5}-α_5 values of 1.061 and 1.067, respectively. The α_{-5}-α_5 value for pedoform B was 0.538, which confirms the lower heterogeneity or entropy of the system in this pedoform, as the smaller the difference between α_{-5}-α_5, the more homogeneous the system (VILLAS-BOAS; CRESTANA; POSADAS, 2014). Therefore, the singularity spectrum quantifies the variability of the PR measurements in the vertical profiles, as described by Siqueira et al. (2013).

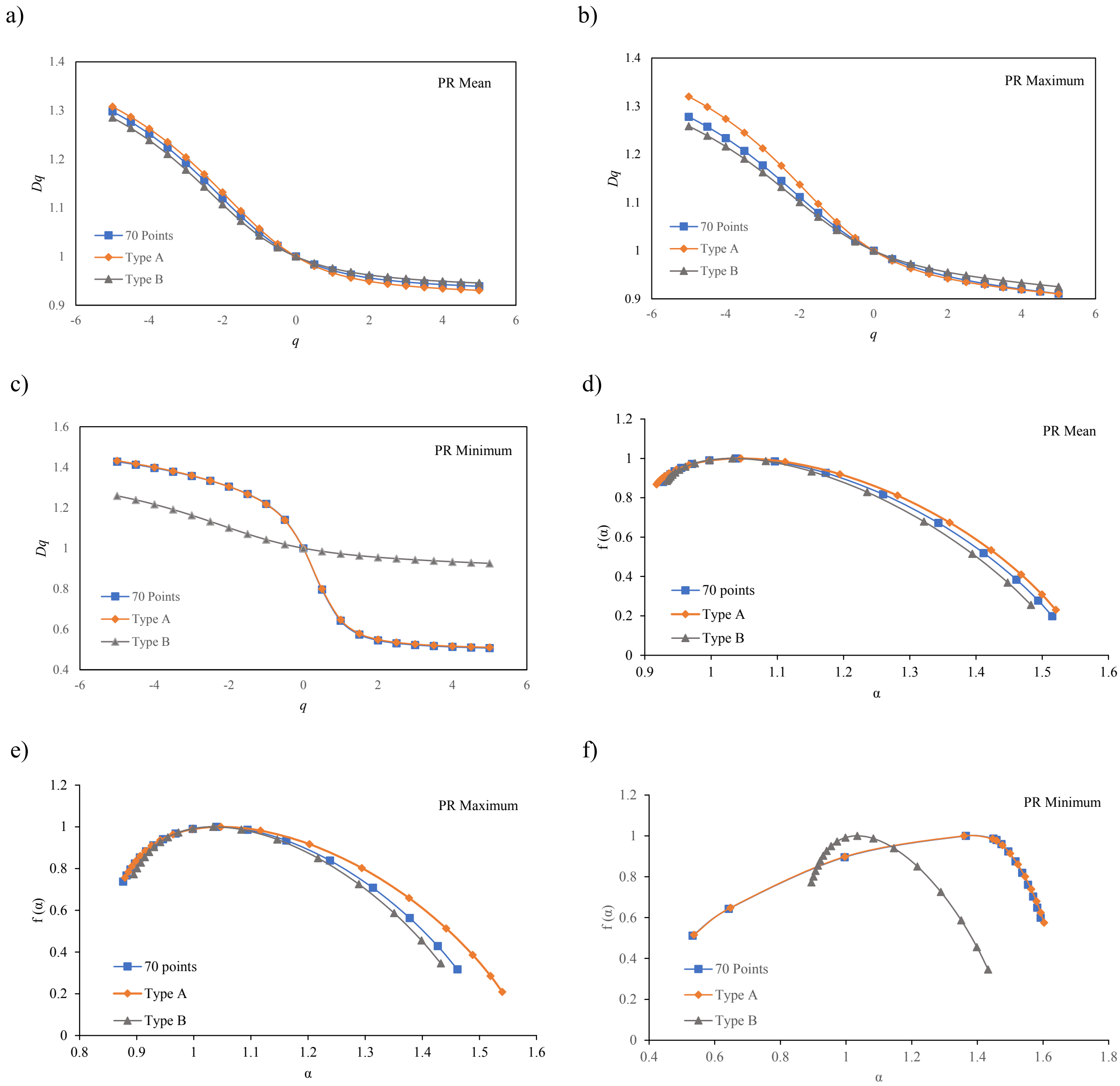

Figure 4. Generalized dimension (a, b, and c) and singularity spectrum (d, e, and f) for the vertical profiles of soil resistance to penetration.

The multifractal parameters of the PR data series showed that the data variability of the different pedoforms was distinct, where the Type A (concave) pedoform was more heterogeneous than the Type B (convex) pedoform. According to Artur et al. (2014), the pedoform influences the intensity and direction of the water flow in the soil, thus justifying the greater scale heterogeneity of low PR values. Rassol, Gaikwad and Talat (2014) studied the influence of the slope forms on the spatial variability of the physical and chemical attributes of the soil, and found that hillside areas have greater variability compared to other slope forms. In terms of soil management, the presence of greater scale heterogeneity related to the $PR_{minimum}$ values demonstrates that monitoring the soil compaction status must consider not only the $PR_{maximum}$ values but also the dynamics of the $PR_{minimum}$ values, as these values are more susceptible to long-term compaction. This corroborates the results of SEIDEL et al. (2018), who described that the proper management of the compaction state favors crop development and an increased crop yield.

On the other hand, the multifractal analysis of all vertical PR profiles (70 points) demonstrated that the $PR_{minimum}$ values in pedoform A underestimated the average values for the 70 sampling points (Figure 4f). According to the singularity spectrum, the minimum PR values for the 70 sampling points and pedoform A have a different behavior in relation to those of pedoform B. This result is important as it demonstrates that the adequate monitoring of the state of compaction must consider the largest number of points possible, faithfully representing zones with greater compaction and regions with a greater compaction tendency.

CONCLUSIONS

The multifractal analysis allowed us to identify differences in the scale variability for the PR measurements in the concave and convex pedoforms, demonstrating its potential for the determination of specific management zones.

The concave pedoform (Type A) had differences regarding the measurement values along the PR profile that would not be detected by conventional analysis methods.

The $PR_{minimum}$ of the different slope forms showed the greatest multifractality of the data, presenting greater scale variation.

The generalized dimension and singularity spectrum proved to have the greatest scale heterogeneity for the concave slope (Type A), which demonstrates that multifractal analysis is efficient in ascertaining the differences in vertical PR profiles along a landscape, allowing the delimitation of management zones considering scale variability.

ACKNOWLEDGMENTS

The authors would like to thank the Fundação de Amparo à Pesquisa e ao Desenvolvimento Científico e Tecnológico do Maranhão (FAPEMA – Processo UNIVERSAL-001160/17 e BD-02105/17). This study was carried out with the support of the Coordenação de Aperfeiçoamento de Pessoal de Nível Superior - Brasil (CAPES) - Financing Code 001 and the Conselho Nacional de Desenvolvimento Científico e Tecnológico (CNPq - Processo 429354/2016-9, 307619/2016-8 e 103961/2018-6).

REFERENCES

ARTUR, A. G. et al. Variabilidade espacial dos atributos químicos do solo, associada ao microrrelevo. **Revista Brasileira de Engenharia Agrícola e Ambiental** 18: 141-149, 2014.

BANERJEE, S. et al. Spatial relationships between leaf area index and topographic factors in semiarid grasslands. Joint multifractal analysis. **Australian Journal of Crop Science**, 5: 756-763, 2011.

BURR-HERSEY, J. E. et al. The developmental morphology of cover crop species exhibits contrasting behavior to changes in soil bulk density, as revealed by X-ray computed tomography. **PLOS ONE**, 12: e0181872, 2017.

CHHABRA, A.; JENSEN, R. V. Direct determination of the f(α) singularity spectrum. **Physical Review Letters**, 62: 12-15, 1989.

CORTEZ, J. W. et al. Spatialization of soil resistance to penetration for localized management by precision agriculture tools. **Engenharia Agrícola**, 38: 690-696, 2018.

DAFONTE-DAFONTE, J. et al. Assessment of the spatial variability of soil chemical properties along a transect using multifractal analysis. **Cadernos do Laboratório Xelóxico de Laxe**, 38: 11-24, 2015.

EVERTSZ, C. J. G.; MANDELBROT, B. B. Multifractal measures. In: Peitgen, H-O.; Jürgens, H, Saupe, D. (Eds.) **Chaos and fractals**. New York: Springer, 1992. v. 1, p. 922-953.

GOOVAERTS, P. Geostatistical tools for characterizing the spatial variability of microbiological and physicochemical soil properties. **Biology and Fertility of Soils**, 27: 315-334, 1998.

HENTSCHEL, H. G. E.; PROCACCIA, I. An infinite number of generalized dimensions of fractals and strange attractors. **Physica D: Nonlinear Phenomena**, 8: 435-444, 1983.

KRAVCHENKO, A. N.; PACHEPSKY, Y. A. Soil variability assessment using fractal techniques. In: Álvarez-Benedí J.; Munoz-Carpena R. (Eds.). **Soil-Water-Solute Process Characterization**: An Integrated Approach. London: CRC Press. 2004. v. 1, cap. 17, p. 617-638.

LEÃO, M. G. et al. Terrain forms and spatial variability of soil properties in an area cultivatedwith citrus. **Engenharia Agrícola**, 31: 643-651, 2011.

LEIVA, J. O. R. et al. Multifractal analysis of soil penetration resistance under sugarcane cultivation. **Revista Brasileira de Engenharia Agrícola e Ambiental**, 23: 538-544, 2019.

LOGSDON, S. D.; PERFECT, E.; TARQUIS, A. M. Multiscale soil investigations: physical concepts and mathematical techniques. **Vadose Zone Journal**, 7: 453-455, 2008.

MORATÓ, M. C. et al. Multifractal analysis of soil properties: spatial signal versus mass distribution. **Geoderma**, 287: 54-65, 2017.

R Core Team. R: a language and environment for statistical computing. Vienna: **The R Project for Statistical Computing**, 2018. Disponível em: <https://www.r-project.org>. Acesso em: 16 out. 2018.

RASSOL, S. N.; GAIKWAD, S. W.; TALAT, M. A. Relações entre propriedades do solo e segmentos de encosta da bacia hidrográfica de wullarhama sallar na bacia hidrográfica de Liddar de Jammu e Caxemira. **Asian Journal of Engineering Research**, 2: 1-10, 2014.

ROISIN, C. J. C. A multifractal approach for assessing the structural state of tilled soils **Soil Science Society of America Journal**, 71: 15-25, 2007.

SANTOS, H. G. et al. **Sistema brasileiro de classificação de solos -SiBCS**. 5. ed. Rio de Janeiro, RJ: EMBRAPA, 2018. 590 p.

SEIDEL, E. P. et al. Soybean yield, soil porosity, and soil penetration resistance under mechanical scarification in no-tillage systems. **Journal of Agricultural Science**, 10: 268-277, 2018.

SIQUEIRA, G. M. et al. Multifractal analysis of vertical profiles of soil penetration resistance at the field scale **Nonlinear Processes in Geophysics**, 20: 529-541, 2013.

SIQUEIRA, G. M. et al. Multifractal and joint multifractal analysis of general soil properties and altitude along a transect. **Biosystems Engineering**, 168: 105-120, 2018.

SOUZA, G. S et al. Controlled traffic and soil physical quality of oxisol under sugarcane cultivation. **Scientia Agricola**, 72: 270-277, 2015.

VIDAL-VÁZQUEZ, E. et al. Multifractal analysis of soil properties along two perpendicular transects **Vadose Zone Journal** 12: vzj2012.0188, 2013.

VILLAS-BOAS, P. R.; CRESTANA, S.; POSADAS, A. Modelagem e simulação. In: Naime, J. M. et al. (Eds.). **Conceitos e aplicações da Instrumentação para o Avanço da Agricultura.** 1. ed. Brasília, DF: EMBRAPA, 2014. v. 1, cap. 13, p. 359-388.

WILSON, M. G. et al. Multifractal analysis of vertical profiles of soil penetration resistance at varying water contents. **Vadose Zone Journal**, 15: 1 -10, 2016.